Eur Biophys J (2008) 37:961–973
DOI 10.1007/s00249-008-0314-z

ORIGINAL PAPER

Spectroscopic and calorimetric studies on the interaction of human serum albumin with DPPC/PEG:2000-DPPE membranes

Manuela Pantusa · Luigi Sportelli · Rosa Bartucci

Received: 22 January 2008 / Revised: 13 March 2008 / Accepted: 13 March 2008 / Published online: 4 April 2008

Abstract Site specific spectroscopic techniques and differential scanning calorimetry were used to study human serum albumin (HSA) in the absence and in the presence of membranes composed of dipalmitoylphosphatidylcholine (DPPC) and poly(ethylene glycol:2000)-dipalmitoylphosphatidylethanolamine (PEG:2000-DPPE). Electron spin resonance (ESR) of a maleimide spin-label (5-MSL) covalently bound to the free sulfhydryl group at the unique cystein Cys-34 in domain I, intrinsic fluorescence of the single tryptophan Trp-214 in domain II, and extrinsic fluorescence of *p*-nitrophenyl anthranilate conjugated with tyrosine Tyr-411 in domain III were employed to study HSA dispersions with or without polymer-grafted membranes. On adsorbing at the DPPC membrane surfaces, domain I assumes a more loosened conformation and partitioning of the spin-labelled protein between the aqueous phase and the interfacial region of lipid membranes is observed by ESR. Domain II and III undergo a local structural arrangement which leads Trp-214 and Tyr-411 to come closer and causes intrinsic fluorescence quenching. The influence of DPPC bilayers on HSA is characterized both by a decrease of the thermal unfolding enthalpy and by a slight increase of the transition temperature, T_t, of the protein. The lipid induced effects on HSA are progressively reduced on increasing the amounts of PEG:2000-DPPE mixed with DPPC from the mushroom regime to the brush regime. Primary protein adsorption at the lipid surfaces is abolished at 1 mol% of the polymer-lipid, whereas the secondary protein adsorption at the polymer-brush leads to a further increase of both transition enthalpy and T_t relative to the case of aqueous dispersions of HSA alone.

M. Pantusa · L. Sportelli · R. Bartucci (✉)
Dipartimento di Fisica, Laboratorio di Biofisica
Molecolare and UdR CNISM, Università della Calabria,
87036 Arcavacata di Rende (CS), Italy
e-mail: bartucci@fis.unical.it

Introduction

The molecular interactions at the lipid/protein interface play an important role not only in regulating the structure/function relationship in cell membranes but also in a variety of relevant biophysical aspects. Recently, many efforts have been devoted to the development of surface coatings to enhance the biocompatibility and bioavailability of materials used in biotechnological and medical applications. For example, in the field of drug delivery, the lifetime of liposome-based drug carriers has been substantially increased by inclusion of lipids with hydrophilic polymer headgroups in the vesicle membranes (Lasic 1993; Lasic and Martin 1995; Lasic and Needham 1995). Phosphatidylethanolamines derivatised by poly(ethylene glycol) of different degree of polymerization (PEGs-PEs) have proved to be particularly useful grafted lipids for producing such sterically stabilized liposomes. Depending on their formulation, the long circulating liposomes inhibit liposome–liposome aggregation, resist protein adsorption, avoid cellular adhesion, avoid diverse elements of the immune system and show efficient release at the target site.

In this context, it is of interest to study the interaction between polymer-grafted membranes and serum proteins. Many studies have addressed the theoretical aspects of the interaction of polymer-modified surfaces with proteins (Jeon et al. 1991; Jeon and Andrade 1991; Szleifer 1997; Halperin 1999; Fang et al. 2005; Fang and Szleifer 2006) and several experimental investigations have considered the mutual influence between polymer-tethered membranes and serum proteins (Du et al. 1997; Efremova et al. 2000; Chiu et al. 2001; Price et al. 2001; Bartucci et al. 2002; Norde and Gage

2004; Bosker et al. 2005; Pantusa et al. 2005; Hashizaki et al. 2006; Dos Santos et al. 2007). In the present work, we study the most abundant plasma protein, human serum albumin (HSA), both in the absence and in the presence of mixed membranes composed of common diacyl lipids of dipalmitoylphosphatidylcholine (DPPC) and sub-micellar amounts of the polymer-lipids dipalmitoylphosphatidylethanolamine bearing on the polarhead PEG of average molecular weight 2,000 Da (PEG:2000-DPPE), which have the same acyl chain length of the parent phospholipids. Our aim is to focus on the molecular effects exerted on the protein by the polymer-grafted membranes. PEG:2000-DPPE is one of the most used PEG-grafted lipids for steric stabilization of phosphatidylcholine liposomes (Lasic and Needham 1995).

HSA is a 66 kDa multifunction protein that contributes significantly to the blood osmotic pressure and to transport and regulatory processes in the circulatory system (Peters 1995). It is a monomeric protein of 585 residues containing 67% of α-helix and 17 disulfide bridges. In its tertiary structure it is possible to distinguish three structurally similar domains I–II–III, each of them further divided into subdomains a and b (see Fig. 1a) (He and Carter 1992; Carter and Ho 1994; Sugio et al. 1999). HSA contains a single free sulfhydryl group at the cysteine residue at position 34 (Cys-34) in the loop connecting two helices in the N-terminal region of domain I, one tryptophan residue at position 214 (Trp-214) in domain II, and a particularly reactive phenolic side chain at the tyrosine residue at position 411 (Tyr-411) in domain III (see Fig. 1a). Exploiting these properties, the three domains of HSA have been investigated by electron spin resonance (ESR) and fluorescence spectroscopies. Indeed, ESR of site-specific covalent labelling of the -SH group of Cys-34 with a maleimide nitroxide derivative (5-MSL), intrinsic fluorescence of the Trp-214 and extrinsic fluorescence of nitrophenyl anthranilate (NPA) conjugated with Tyr-411 (see Fig. 1b), have contributed to gain insight into the molecular properties of aqueous dispersions of HSA both in the absence and in the presence of PEG:2000-DPPE grafted DPPC membranes. The interaction of HSA with PEG:2000-grafted DPPC membranes has been further investigated by means of differential scanning calorimetry (DSC).

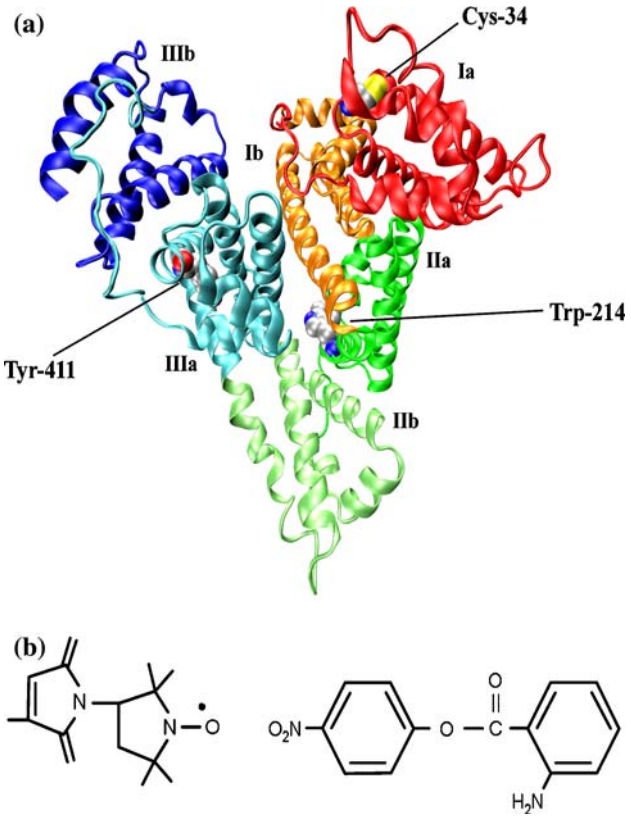

Fig. 1 **a** Crystal structure of HSA (23; PDB code: 1AO6) indicating the regions around Cys-34 in the domain I, around Trp-214 in domain II, and around Tyr-411 in domain III. **b** Structures of the maleimide spin label 5-MSL (*left*) and of the fluorescent label NPA (*right*) used for the covalent labelling of HSA at the free SH-group of Cys-34 and at the Tyr-411 residue, respectively

Materials and methods

Chemicals

Essentially fatty acid-free and globulin-free human serum albumin (HSA, type A-3782, purity approximately 99%), the synthetic lipid 1,2-dipalmitoyl-*sn*-glycero-3-phosphatidylcholine (DPPC), the maleimide spin label 3-maleimido-2,2,5,5-tetramethyl-1-pyrrolidinyloxy (5-MSL) and the polymer poly(ethylene glycol)methyl ether with average molecular weight 2,000 (PEG:2000) were from Sigma/Aldrich (St Louis, MO). *p*-Nitrophenyl anthranilate (NPA) was purchased from Fluorochem (Derbyshire, UK). High-purity (>99%) PEG-lipid 1,2-dipalmitoyl-*sn*-glycero-3-phosphoethanolamine-*N*-poly(ethylene glycol) with PEG of average molecular mass 2,000 Da (PEG:2000-DPPE) was obtained from Avanti Polar Lipids (Birmingham, AL). The reagent grade salts for the 10 mM phosphate buffer solution (PBS) at pH 7.2 were from Merk (Darmstadt, DE). All materials were used as purchased with no further purification. Distilled water was used throughout.

ESR

Spin-labelled protein. Dispersions of HSA spin labelled covalently on the single free cysteine residue, Cys-34, by reaction with the maleimide spin-label, 5-MSL, were prepared as follows. A volume of methanol containing the spin label was first evaporated under a flow of nitrogen gas and any residual solvent removed under vacuum. A buffered HSA solution was then added to the dried spin label. The

spin-label concentration was fivefold molar excess with respect to the protein concentration. The mixture was incubated for 24 h at 4°C with gentle stirring. Excess free spin label was finally removed from the spin-labelled protein solution by exhaustive dialysis at 4°C against PBS (10 mM, pH 7.2) until no free spin-label was detected in the ESR spectra of the dialysis medium. This procedure ensures that all the spin-label is covalently bound to the protein on Cys-34. Protein concentration was determined spectrophotometrically and was adjusted to 0.6 mM with PBS for ESR measurements.

Spin-labelled protein/lipid mixtures. Samples for the ESR measurements on the spin-labelled protein in the presence of DPPC/PEG-grafted lipid dispersions were prepared dissolving the required amounts of DPPC and PEG:2000-DPPE in chloroform–methanol and evaporating off the solvent first in a nitrogen gas stream and then under vacuum overnight. The dried lipid samples were fully hydrated with the spin labelled HSA buffered solution by heating at 45°C, i.e., above the chain-melting transition temperature of the lipids, and periodically vortexing for 30 min. In any dispersion, the final lipid concentration was 54 mM and the protein/lipid ratio was 1:1 w/w. All the samples were transferred in ESR glass capillaries (1 mm i.d., 100 μL), flame sealed and stored overnight at 4°C before the ESR measurements.

ESR measurements. ESR spectra were acquired on an ESP-300 9-GHz spectrometer (Bruker, Karlsruhe, DE). The sample capillary was inserted in a standard 4 mm diameter ESR quartz tube containing light silicon oil for thermal stability and centred in a Bruker ER 4201 rectangular TE_{102} ESR cavity. Sample temperature was controlled with a Bruker Euroterm ER 4111VT variable temperature control unit (accuracy ± 0.1°C). Conventional, in-phase, absorption ESR spectra were recorded well below saturation at a microwave power of 10 mW using a 100 kHz field modulation frequency for phase sensitive detection and 1 $G_{p\text{-}p}$ as amplitude of the magnetic field modulation signal.

Data analysis. The ESR spectra of 5-MSL in HSA in the absence and in the presence of PEG:2000-grafted membranes consist of two spectral components corresponding to spin-label populations with different mobility on the conventional ESR time scale. The labels with greater mobility give rise to a nearly isotropic triplet, referred to as weakly immobilized component, *W*, and those with more restricted motion contribute with an anisotropic pattern, referred to as strongly immobilized component, *S* (see Fig. 2b). To determine the *S* and *W* contributions, the composite spectra were resolved into the *S* and *W* components by spectral subtraction as described in (Griffith and Jost 1976; Jost and Griffith 1976; Marsh 1982). Briefly, by subtracting from the composite spectrum an appropriate weakly *W* (strongly *S*) immobilized signal, the strongly *S* (weakly *W*) component difference spectrum can be obtained. In our case, a single component spectrum (either *S* or *W* signal) necessary for the subtractions has been obtained either experimentally or has been simulated at each temperature using WIN-EPR, SimFonia software program, Version 1.2 from Bruker. Once the *S* and the *W* components are resolved, by taking into account the double integral of the original spectra, the spin-label populations of the weakly, N_W, and of the motionally restricted, $N_S = 1 - N_W$, spin-label populations were determined.

The *S* and *W* spectral components were analyzed by means of the outermost hyperfine splitting separation, $2A_{max}$, and of the peak-to-peak linewidth of the low-field hyperfine manifold, ΔW_{+1}, respectively (see Fig. 2c). These are spectral parameters that characterize the dynamics of spin-labelled biosystems (Marsh 1981; Marsh and Horvath 1989, 1998). The temperature dependence of the label populations was used to monitor conformational changes in the spin-labelled HSA in the absence and in the presence of lipid membranes. The ESR data points are the average ± standard deviations of triplicate measurements.

Fluorescence

Sample preparation. For intrinsic Trp fluorescence measurements, HSA was dispersed in PBS at pH 7.2. The same solution was also used to hydrate lipid/polymer-lipid dry films prepared as described above for the ESR measurements. Protein concentration was 5 μM and the lipid to protein ratio 1:1 w/w in any sample. Preparation of anthraniloyl-Tyr-411–HSA was accomplished as follows (Hagag et al. 1983). NPA was dissolved in acetonitrile and added in two molar excess to a protein solution in PBS at pH 8.0. The reaction was allowed to proceed for 7 h at room temperature after which the preparation was dialyzed against PBS at pH 7.2 at 4°C to remove the *p*-nitrophenol produced. Appropriate solutions of NPA–HSA complexes were used for hydrating polymer-lipid grafted membranes.

Fluorescence measurements. All fluorescence spectra of HSA and of HSA/polymer-grafted membranes were recorded using a LS 50B spectrofluorometer (Perkin-Elmer, Beaconsfield, UK) equipped with a Peltier Temperature Programmer PTP-1. The excitation wavelength was set at 295 nm (330 nm) and the emission spectra were recorded at 400 nm/min over the range 300–400 nm (350–500 nm) for Trp (NPA), respectively. Both the excitation and emission slits were set at 4 nm. The temperature was scanned at 60°C/h and measured directly by an YSI thermistor dipped into 1 cm path length quartz cuvette. Each spectrum was the average of five scans. The background of light scattering of the buffer as well as that of the phospholipid dispersions was always subtracted. Moreover, the vesicles scattering artefacts, that cause loss of fluorescence

intensity due to the attenuation of excited and emitted light, were corrected using intensity data from non-interacting Trp zwitterion (Ladokhin et al. 2000). The fluorescence measurements were repeated to test their reproducibility.

Differential scanning calorimetry (DSC)

Sample preparation. Samples for DSC measurements were prepared as described above for fluorescence except that the protein concentration was 0.15 mM.

DSC measurements. The calorimetric scans, which give the excess heat capacity at constant pressure (Cp_{exc}) versus temperature, were acquired using a high sensitivity differential scanning calorimeter model VP-DSC (MicroCal Inc., Northampton, MA) with cell volumes of 0.52 mL. To obtain a reproducible baseline, at least four buffer versus buffer scans were performed. After the reference measurements, the sample cell was emptied, reloaded with the sample solution and equilibrated for 50 min at 20°C. The samples were degassed before the scans and the thermograms were recorded on heating with scan rate of 15°C/h.

The calorimetric data were analysed using MicroCal ORIGIN dedicated software (MicroCal Software Inc.). All the Cp_{exc} curves were obtained from the calorimetric profiles baseline corrected (by using a progress baseline) and concentration normalized. Three different samples were measured and the values are the averages ± standard deviations. The molar enthalpy, ΔH, of the protein thermal unfolding transition was obtained from the area under the DSC peak and the concentration of HSA in each sample, whereas the temperature of the transition, T_t, is the temperature at which Cp_{exc} is maximum.

Results

The samples studied in this paper are aqueous dispersions of HSA in the absence and in the presence of DPPC/PEG:2000-DPPE membranes at the protein/lipid ratio of 1:1 w/w. The content of the polymer-lipid mixed with DPPC was varied between 0 and 2 mol%, a submicellar concentration range that encompasses the mushroom → brush transition of the polymer chains. For gel phase DPPC bilayers and PEG:2000-lipids, this transition theoretically is predicted at 0.9 mol% of the polymer-lipid whereas experimentally was found to occur at ≈1.5 mol% (Bartucci et al. 2002; Marsh et al. 2003). Moreover, optimal plasma circulation time is achieved with liposomes containing 2 mol% of PEG:2000-lipids (Dos Santos et al. 2007).

ESR measurements

Spin-labelled HSA

At any temperature, the ESR spectrum of 5-MSL in PBS at pH 7.2 consists of an isotropic triplet indicating that the motion of the label lies on the fast motional regime of the conventional ESR time scale (rotational correlation time $\tau_c < 3 \times 10^{-9}$ s) (Marsh 1981). In Fig. 2a the spectrum at 20°C is reported. At the same temperature, the spectrum of the label covalently bound to the SH-group of Cys-34 in human serum albumin dispersed in buffer solution clearly consists of two components with different motional sensitivity (Fig. 2b). Indeed, an outer, strongly immobilized spectral component, *S*, and an inner, more mobile, weakly immobilized signal, *W*, are evident in the ESR spectrum of the spin-labelled HSA. They overlap mainly in the central region of the spectrum, corresponding to the $M_I = 0$ hyperfine

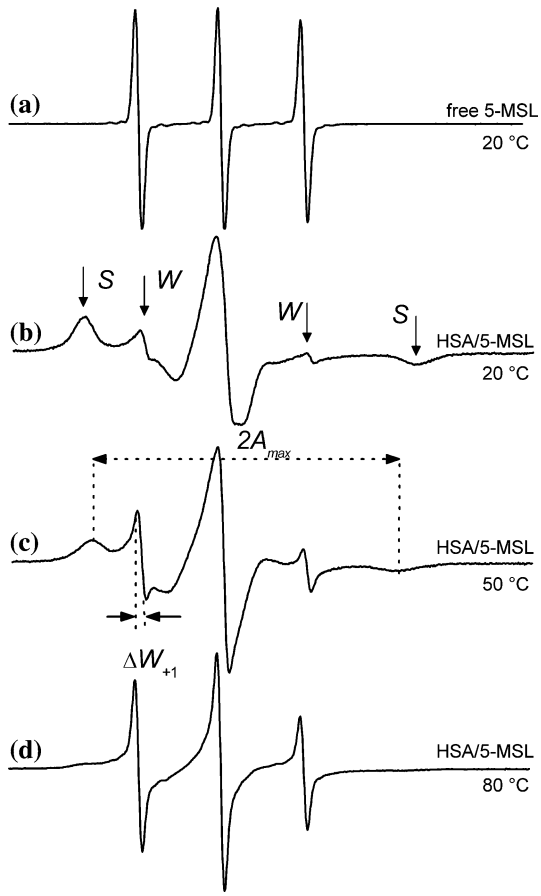

Fig. 2 ESR spectra of free 5-MSL in PBS at 20°C (**a**), of 5-MSL covalently bound to HSA in PBS at 20 (**b**), 55 (**c**) and 80°C (**d**). The *arrows* indicate the outermost lines of the strongly immobilized, *S*, and the weakly immobilized, *W* components; $2A_{max}$ is the outermost peak separation of the *S* component, whereas ΔW_{+1} represents the peak-to-peak linewidth of the $M_I = +1$ hyperfine manifold of the *W* component. Total scan range 100 G

manifold. This allows estimation of the outermost hyperfine peak separation of both components. The outer hyperfine splitting, $2A_{max}$, of the strongly immobilized component, which reflects the probe mobility, is >64 Gauss at 20°C. This high $2A_{max}$ value indicates that the motion of the label covalently bound to the Cys-34 protein residue is restricted. The outer hyperfine separation of the *W* component, which is a parameter sensitive to the environmental polarity, is 31.80 G. It is similar to that of the free spin-probe in PBS (31.84 G) (Fig. 2a) and maintains this value up to 80°C. The results, therefore, suggest that the protein region around Cys-34, where the maleimide probe is bound, is exposed to the solvent. Accessibility of the solvent to Cys-34 in HSA has been demonstrated directly by electron spin echo envelope modulation experiments (De Simone et al. 2007) and by fluorescence using acylodan, a cystein specific fluorescent probe (Narazaki et al. 1997).

Two spectral components are recorded in the whole temperature range investigated (20–80°C) whose relative contribution to the ESR spectra depends on temperature (see spectra c, d at 55 and 80°C, respectively, in Fig. 2). Indeed, on increasing the temperature the *S* component becomes less intense and the *W* component increases. This latter dominates the spectra at the highest temperatures, although a residual contribution of the *S* component is always evident (see spectrum at 80°C in Fig. 2d).

HSA was also spin-labelled at Cys-34 with the maleimide derivative probe 3-[2-(2-maleimidoethoxy)ethyl-carbamoyl]-PROXYL having a longer space between the point of attachment at the protein and the nitroxide ring. In these samples, at any temperature the mobile *W* component is much more intense than the *S* component and from 70°C onwards the spectra show only the *W* component. It is known that for MSLs the *S* component is progressively reduced on increasing the length of the spin probe (Graceffa and Lehrer 1984; Sterk et al. 1994).

In HSA solution at pH 6.0–7.0, maleimide spin labels react solely with the free SH group of Cys-34 located in a crevice on the protein surface, whose configuration is not rigid and undergoes a transition between two conformational states (Wetzel et al. 1980). The spin-labels are, therefore, distributed over two different environments arising from two distinct temperature-dependent equilibrium conformations. Our experimental results suggest that the immobilized component arises from labels that are buried in the Cys-34 cavity and their restricted motion reflects the segmental motion of the backbone relative to the average protein structure. The mobile component, instead, is contributed by labels bound to the protein in a more loosened state. They posses more freedom of motion related to rotational isomerisation around the bond that link the nitroxide ring to the protein.

Spin labelled HSA in the presence of DPPC dispersions

When aqueous spin-labelled protein solutions are used to hydrate DPPC bilayers, composite ESR spectra are still obtained (Fig. 3a–c). However, the following interesting differences relative to the previous case of HSA/5-MSL can be evidenced: (1) at any temperature up to 50–55°C, the relative population of the two *S* and *W* components changes (see also later Fig. 4b). For example, comparing the spectrum at 20°C in Fig. 3a with the corresponding one in Fig. 2b, it appears that the intensity of the *W* component is higher in the presence of DPPC bilayers; (2) on increasing the temperature from ca. 30–35°C, the high field line of the *W* component shows two distinct peaks (see spectra at 55 and 80°C in Fig. 3b, c; respectively). These latter are also evident in the corresponding spectra of the free 5-MSL in the presence of DPPC dispersions given in Fig. 3e, f, whereas they are not resolved at the lowest temperature up to ca. 30–35°C (see spectrum at 20°C in Fig. 3d). The most likely explanation of the above results is that the *W* component is the overlap of two isotropic signals due to the

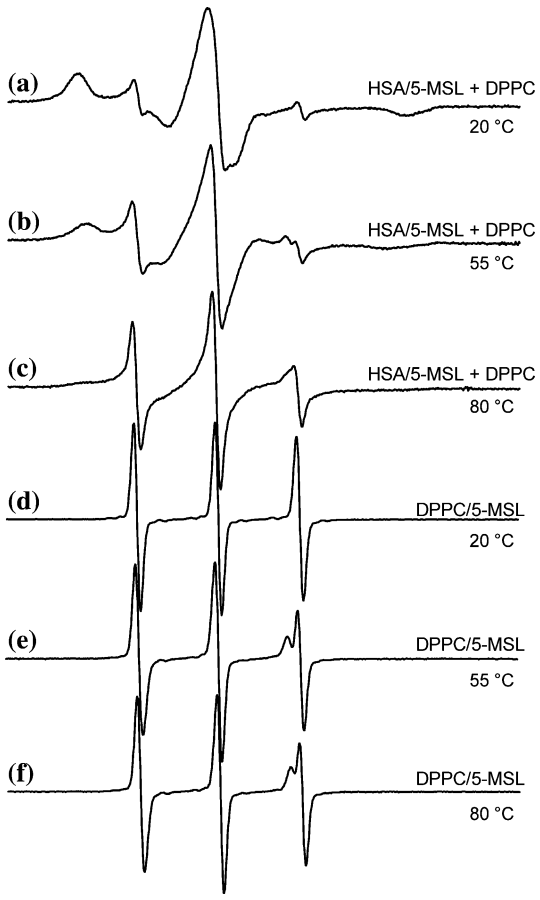

Fig. 3 ESR spectra of 5-MSL covalently bound to HSA in the presence of DPPC dispersions at 20 (**a**), 55 (**b**) and 80°C (**c**). ESR spectra of 5-MSL in aqueous DPPC bilayers at 20 (**d**), 55 (**e**) and 80°C (**f**). Total scan range 100 G

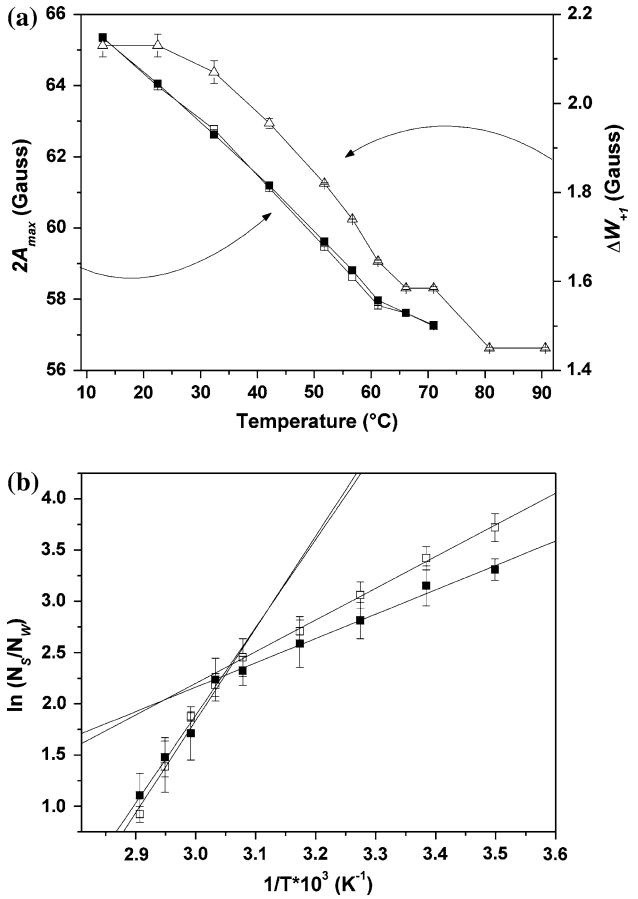

Fig. 4 Temperature dependence of ESR parameters of 5-MSL covalently bound to HSA. **a** Temperature dependence of the outermost peak separation, $2A_{max}$, of the *S* component (*squares*) and of the peak-to-peak linewidth at low field, ΔW_{+1}, of the *W* component (*triangles*); **b** Population ratio, N_S/N_W, of the strongly and weakly immobilized components versus $1/T$. *Open symbols* refer to aqueous dispersions of spin-labelled HSA and *solid symbols* to spin-labelled HSA in the presence of DPPC dispersions

partitioning of the labelled protein between the aqueous and membrane phases. As membranes have higher viscosity and lower polarity than water, there are small differences in the isotropic hyperfine splittings, A_0, and g values. Thus, at 9 GHz only the resonance lines at high field are resolved. First the signal in the membrane and then the one in water are evident. This is what is normally found when small spin-label molecules partition between the aqueous and membrane phases in studies on fluidity, lateral phase separations and phase transitions in lipid membranes (Marsh 1981). In our study, for both samples, i.e., 5-MSL bound to HSA and free 5-MSL, the label partitioning in DPPC multilayers becomes appreciable from 30 to 35°C onwards and reaches a plateau at ca. 60–65°C. The degree of partitioning is, however, limited and, given the extent of the separation of the two components, it is likely that the labelled protein inserts in the interfacial headgroup region of the DPPC bilayers. A better resolution of the two signals would be expected for a spin probe able to partition deeper in the hydrocarbon region of lipid bilayers (Marsh 1981). The spectra reported in Fig. 3a–c, therefore, give a clear evidence of the interaction of HSA with DPPC bilayers at the interface: in the presence of DPPC bilayers, the labels contributing to the *W* component interact with the lipid bilayers.

The effects of DPPC on spin-labelled HSA can also be determined by separating the *S* and *W* components by spectral subtraction (see "Materials and methods") and analyzing the temperature dependence of the outer hyperfine splitting of the strongly immobilized component, $2A_{max}(S)$, and when appropriate, of the linewidth at low field of the weakly immobilized component, $\Delta W_{+1}(W)$. The *S* component is an anisotropic powder pattern typical of labels in the slow motion regime on the conventional ESR timescale. Instead, the *W* component consists of three lines with different height and differential broadening indicative of labels with reduced freedom of motion relative to that of free 5-MSL both in buffer and in the presence of DPPC bilayers at low temperature. For HSA/5-MSL aqueous dispersions, the $2A_{max}(S)$ values (open squares in Fig. 4a) decrease continuously, first rapidly and then more slowly from 60°C onwards. The $2A_{max}$ values suggest that the protein gains some motion on increasing the temperature and when the unfolded state at ca. 60–65°C (see later DSC results) is approached. $\Delta W_{+1}(W)$ values (open triangles in Fig. 4a) decreases from 2.1 to 1.4 G between 10 and 80°C, whereas those of free 5-MSL in buffer (data not shown) maintain a constant value of 1.3 G in the same temperature range. The temperature decrease of $\Delta W_{+1}(W)$ indicates that the motion of 5-MSL weakly immobilized to HSA becomes progressively more rapid with temperature increase and it is restricted relative to that of free label in water.

The presence of DPPC bilayers does not influence the temperature dependence of $2A_{max}(S)$ (solid squares in Fig. 4a). This indicates that DPPC bilayers do not induce local structural alteration in the HSA region around Cys-34 probed by labels contributing to the *S* signal.

Since for HSA/5-MSL in the presence of DPPC bilayers the *W* component is contributed by two isotropic signals as the temperature increases, it is not appropriate to analyze the temperature profile of $\Delta W_{+1}(W)$. However, at low temperature, as long as there is no partitioning into the membrane, the spin-labelled protein population of the *W* component has higher freedom of motion with respect to the case of HSA/5-MSL, which in turn is restricted relative to free 5-MSL in buffer and/or in lipid dispersions. Indeed, between 10 and 25°C, $\Delta W_{+1}(W)$ decreases from 2.1 to 1.7 G (data not shown) on going from HSA to (HSA + DPPC) samples, whereas ΔW_{+1} is 1.3 G for free 5-MSL in lipid membranes. The results indicate that DPPC bilayers promote a loosened protein conformation around Cys-34 in domain I of HSA.

In Fig. 4b are compared the ratio, N_S/N_W, of the *S* and *W* label populations for HSA/5-MSL (open symbols, full line) and for HSA/5-MSL + DPPC samples (solid symbols, dashed line) versus $1/T$. Using the Boltzmann distribution for the relationship of spin-labelled populations, $N_S/N_W \propto \exp(\Delta Ea/kT)$, the slope of a least-squares linear fit to the data over the temperature range 10–50°C yields the values for the activation energy of 27.6 ± 0.8 kJ/mol and of 74.9 ± 6.3 kJ/mol between 50 and 70°C for HSA/5-MSL. These values imply a significant conformational change in HSA at a temperature of ≈54.2°C. Relative to the above case of HSA alone, the activation energy is lower for HSA/5-MSL/DPPC complexes between 10 and 55°C (21.3 ± 0.8 kJ/mol), whereas it is almost the same in the high temperature range (71.5 ± 7.9 kJ/mol). Moreover, the presence of DPPC dispersions shifts up of about 1°C the break in the slope of the graph in Fig. 4b, indicating that in the HSA/DPPC complex the protein undergoes a local structural change at a slightly higher temperature.

Spin labelled HSA in the presence of DPPC/PEG:2000-DPPE dispersions

For spin-labelled protein samples in the presence of mixtures of DPPC and submicellar content of PEG:2000-DPPE, the lineshapes of the composite ESR spectra reveal interesting features of the protein/polymer-grafted membranes interaction. The spectra of 5-MSL covalently bound to HSA in the presence of increasing concentration of PEG:2000-DPPE mixed with DPPC show a progressive decrease of the intensity of the *W* component and the spectral lineshapes became similar to that of HSA alone (see inset to Fig. 5). This is also seen in the trend of the plot in Fig. 5 where the ratio of the strongly over the weakly immobilized label populations first increases constantly and then more rapidly reaching a value close to that of HSA/5-MSL sample. Clearly, the polymer coating at the lipid/protein interface progressively attenuates the lipid-induced effects on the protein. In particular, it is worthy to note that the ESR spectra at high temperatures of HSA/5-MSL/(DPPC + 1 mol% PEG:2000-DPPE) (not shown) do not evidence anymore the splitting in the resonance line at high field of the *W* component that was a peculiar spectral characteristic of lipid/protein interaction (see spectra in Fig. 3b, c). These findings support the conclusion that the protein adsorption at the DPPC membrane surfaces (primary adsorption) does not occur anymore in the presence of high concentrations of PEG:2000-DPPE. However, they indicate that the polymer brush affects the protein dynamics and conformation.

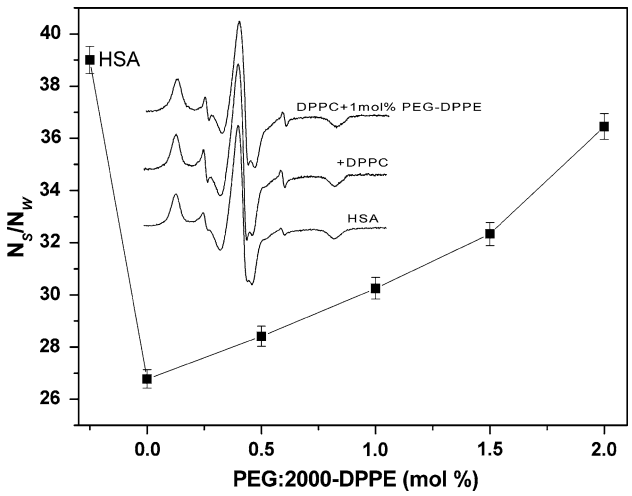

Fig. 5 Dependence of the population ratio, N_S/N_W, of the strongly and weakly immobilized components on the content of the polymer-lipid PEG:2000-DPPE. *Inset* ESR spectra at 10°C of 5-MSL in HSA alone, in the presence of DPPC, and in the presence of DPPC + 1 mol% PEG:2000-DPPE

Fluorescence measurements

Tryptophan fluorescence

The intrinsic fluorescence of HSA comes from the unique tryptophan residue, Trp-214, 19 tyrosine residues and phenylalanine. At the excitation wavelength of 295 nm, the emission spectrum of HSA in PBS at pH 7.2 is almost due to Trp only.

A typical emission Trp spectrum is obtained for buffered aqueous dispersions of HSA at 25°C (Fig. 6, solid line). It exhibits an emission maximum centred at 345 nm, close to the position of the maximum reported for free tryptophan in aqueous solution (348–350 nm) (Lakowicz 1983). This indicates that Trp-214 in the domain II of HSA is exposed to the solvent. The interaction with DPPC membranes leads to a marked decrease of the fluorescence intensity and to a modest blue-shift in the emission of Trp (Fig. 6, bottom dashed line). A better characterization of the protein region around Trp-214 in the absence and in the presence of DPPC membranes is given by the temperature dependence of the maximum fluorescence intensity, F_{max}, and of the maximum wavelength emission, λ_{max}, given in Fig. 7a, b; respectively.

For HSA in PBS, F_{max} undergoes a large decrease (about 60%) with temperature (Fig. 7a, open symbols), whereas λ_{max} is shifted to shorter wavelength (blue shift) of about 10 nm in a sigmoidal fashion with a midpoint at ca. 55°C (Fig. 7b, open symbols). Likely, on increasing the temperature, the domain II of HSA assumes a conformation which favours an intrinsic fluorescence quenching, shields Trp-214 from the aqueous solvent and forces it in a more apolar environment. A reduction in fluorescence intensity paired with a blue shift has previously been observed for HSA subsequent to thermal unfolding (Krishnakumar and Panda

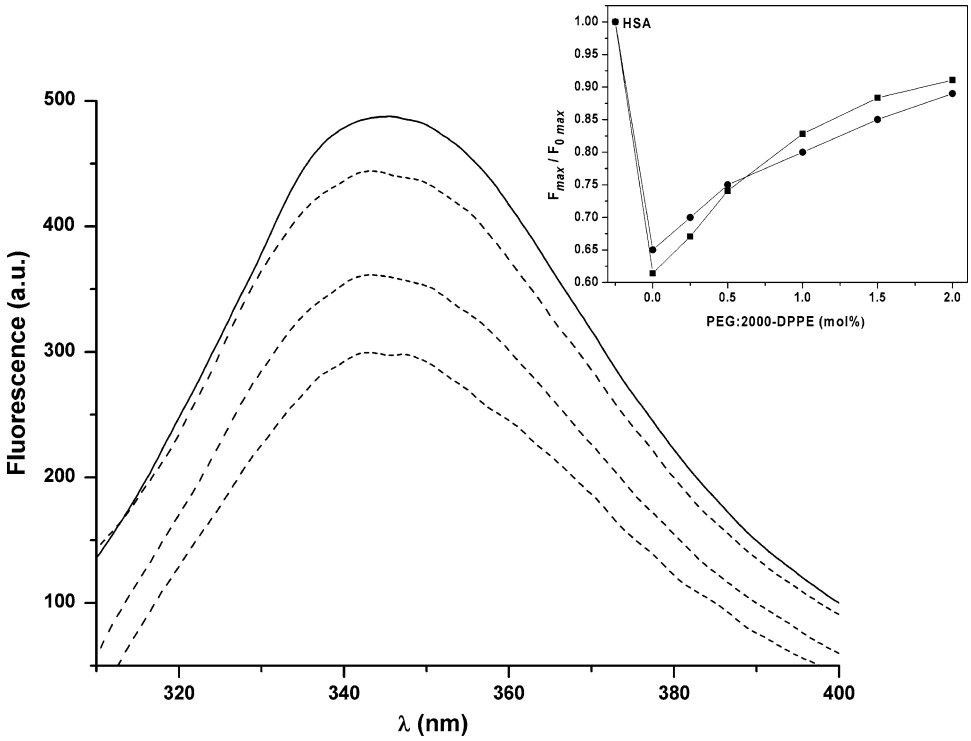

Fig. 6 Fluorescence spectra at 25°C of Trp-214 in HSA dispersions in the absence (*solid line*) and in the presence of dispersions of DPPC, DPPC/0.5 mol% PEG:2000-DPPE, DPPC/2 mol% PEG:2000-DPPE (*dashed lines*, *bottom* to *top*). *Inset* dependence of the ratio of the maximum fluorescence intensity, F_{max}/F_{0max}, on the content of the polymer-lipid PEG:2000-DPPE. F_{0max} is the maximum fluorescence intensity of Trp-214 (*squares*) and of NPA–Tyr-411 (*circles*) in HSA. The *errors* are smaller than the *symbols*

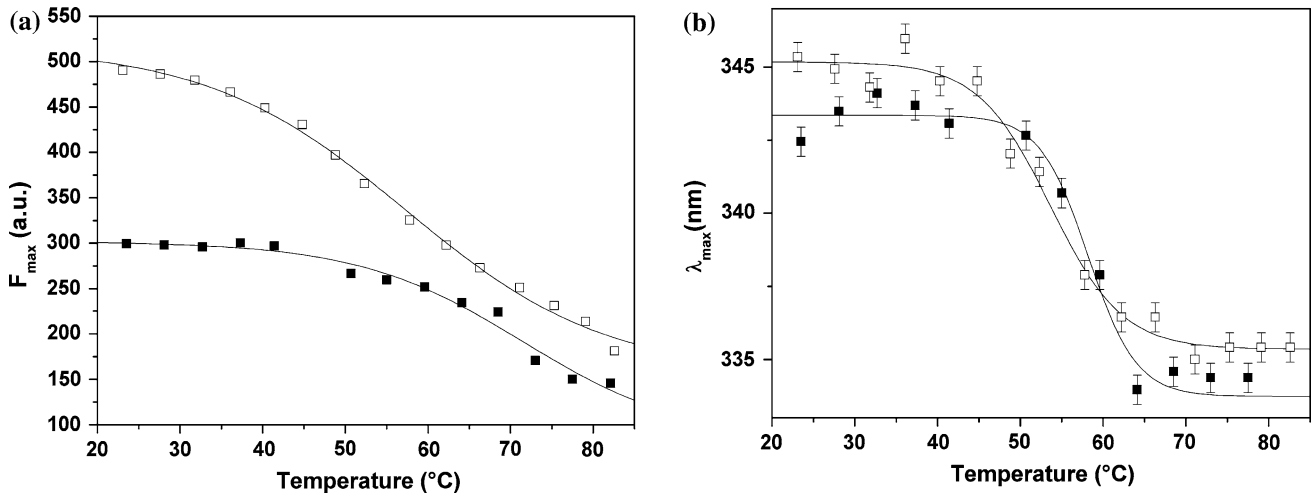

Fig. 7 **a** Temperature dependence of the maximum fluorescence intensity, F_{max}, of Trp-214 in HSA (*open symbols*) and in HSA/DPPC complexes (*solid symbols*). The *errors* are smaller than the *symbols*. **b** Temperature dependence of the maximum wavelength, λ_{max}, for Trp-214 fluorescence spectra in HSA (*open symbols*) and in HSA/DPPC complexes (*solid symbols*)

2002) and chemical denaturation in the pH range 5.4–9.9 (Faruggia and Pico 1999). Moreover, HSA acidic denaturation obtained by lowering the pH from 6 to 2 results in a blue shift, whereas a red shift is seen for HSA in guanidine hydrochloride (Muzammil et al. 1999).

In the presence of DPPC bilayers, the most striking features in Fig. 7a, b (solid symbols) are: (1) a moderate temperature dependence of F_{max}, relatively gradual up to 60°C and then faster; (2) the difference [F_{max}(HSA) − F_{max}(HSA + DPPC)] is large up to 50–55°C (about 100–200 a.u.) and then decreases to about 50 a.u.; (3) DPPC bilayers have little effect on λ_{max}, which is slightly lower than that in HSA dispersions in the whole temperature range with the mid-point slightly upward shifted.

The interaction of HSA with DPPC bilayers causes fluorescence quenching without changing the polarity around the microenvironment of Trp-214. Indeed, a more marked blue shift would be expected for the fluorophore localized in the apolar region of the lipid chains (Ren et al. 1997; Liu et al. 2006).

When buffered HSA solutions are used to hydrate DPPC/PEG:2000-DPPE dispersions, the Trp fluorescence data indicate that the lipid–protein interaction is progressively reduced on increasing the amount of polymer-lipids mixed with DPPC dispersions. This is seen both in the emission spectra in Fig. 6, which approach that of original HSA, and in the recovering of the fluorescence intensity versus polymer-lipid content given in the inset to Fig. 6. However, at the highest concentration of the polymer-lipid, the HSA fluorescence spectrum is not completely recovered, suggesting an influence of the PEG:2000 brush on the protein.

Antranilate fluorescence

The fluorescence data of NPA covalently bound to Tyr-411 in domain III of HSA in the absence and in the presence of DPPC/PEG:2000-DPPE dispersions show differences and similarities with those of the intrinsic Trp-214 fluorescence reported above. A typical fluorescence spectrum of NPA–HSA at 25°C (inset to Fig. 8, solid line) is centred at 410 nm as expected for such a chromophore bound to an amino acid residue in a polar environment (Hagag et al. 1983). Contrary to the Trp fluorescence data, a moderate temperature variation is recorded for F_{max}, which slightly increases when the temperature of protein unfolding is approached (Fig. 8, open symbols). For the same system, λ_{max} has an almost constant temperature value (data not shown) and it is not affected by DPPC/PEG:2000-DPPE membranes at any temperature (see spectrum in dashed line, inset to Fig. 8). Similarly to the Trp fluorescence data, the presence of DPPC bilayers induces a marked decrease of the fluorescence intensity of NPA–HSA, whose temperature variation (Fig. 8, solid symbols) almost mirrors that seen in the protein alone. Fluorescence data of NPA–HSA in the presence of DPPC/PEG:2000-DPPE dispersions also show that the fluorescence intensity progressively recovers, without reaching the reference value of HSA, when increasing amount of polymer-lipids are mixed with DPPC (see circles in the inset to Fig. 6).

DSC measurements

DSC heating scans of aqueous HSA dispersions in the absence and in the presence of DPPC/PEG:2000-DPPE dispersions are shown in Fig. 9. The protein sample (solid line) shows an asymmetric endothermic peak at $T_t = 63.3$°C with an unfolding enthalpy of 820 kJ/mol (see Table 1). The characteristics of the protein thermal unfolding transition are in agreement with literature data under the same experimental conditions used in this study, i.e., protein concentration and purity, ionic strength and pH values of the dispersion medium, scan rate of the measurements (Faruggia and Pico 1999; Pico 1997; Michnik et al. 2005; Shrake et al. 2006). The chemically induced unfolding process of the three domains of HSA, monitored using specific covalently bound fluorescent probes, was found to occur sequentially: the unfolding of domain II and domain III preceded that of domain I (Santra et al. 2005). This is in

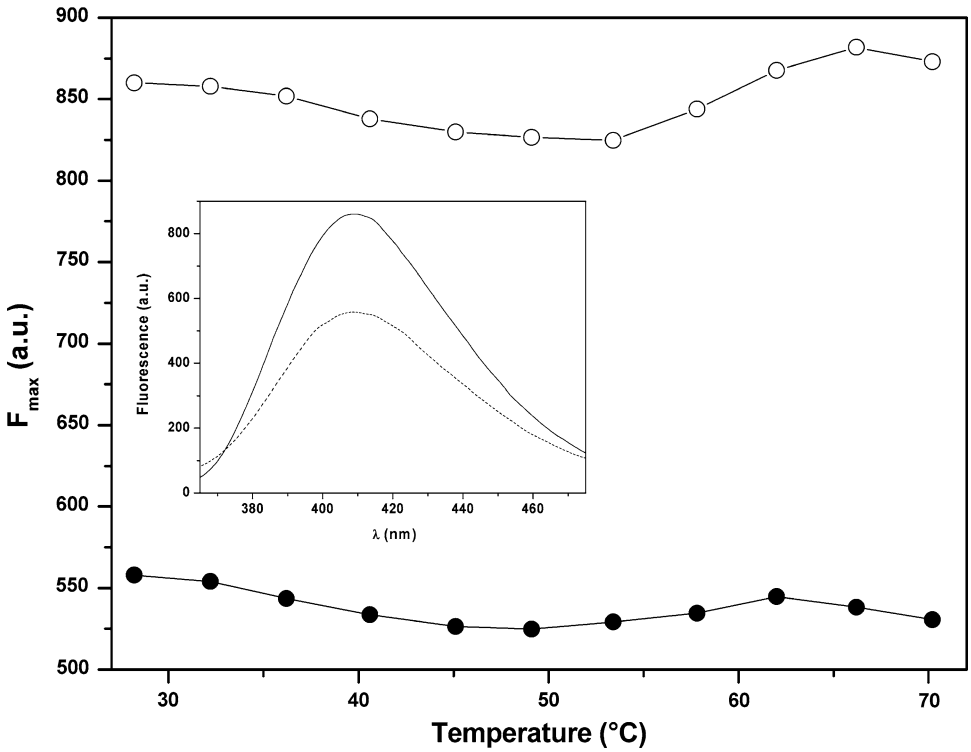

Fig. 8 Temperature dependence of the maximum fluorescence intensity, F_{max}, of NPA–Tyr-411 in HSA (*open symbols*) and in HSA/DPPC complexes (*solid symbols*). The *errors* are smaller than the *symbols*. *Inset* fluorescence spectra at 25°C of NPA–Tyr-411 in HSA dispersions in the absence (*solid line*) and in the presence of DPPC dispersions (*dashed line*)

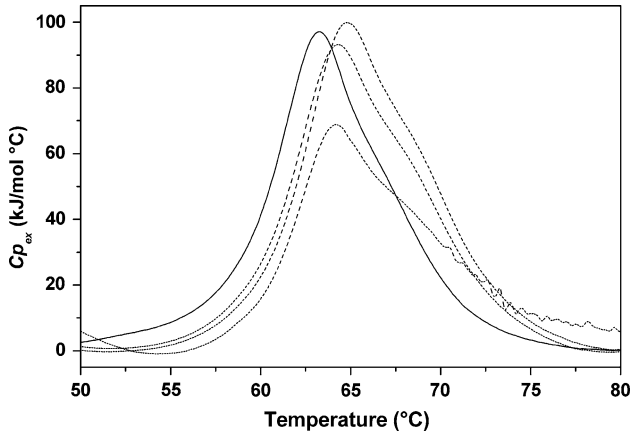

Fig. 9 DSC heating thermograms of HSA dispersions in the absence (*solid line*) and in the presence of dispersions of DPPC, DPPC/0.5 mol% PEG:2000-DPPE, DPPC/2 mol% PEG:2000-DPPE (*dashed lines*, *bottom* to *top*)

Table 1 Thermodynamic parameters for the thermal unfolding of aqueous dispersions of HSA in the absence and in the presence of either DPPC/PEG:2000-DPPE membranes or free PEG:2000

Sample	T_t (°C)	ΔH (kJ/mol)
HSA	63.3 ± 0.1	820 ± 5
+DPPC	64.2 ± 0.1	690 ± 3
+0.5 mol% PEG:2000-DPPE	64.3 ± 0.1	820 ± 4
+1 mol% PEG:2000-DPPE	64.4 ± 0.1	820 ± 3
+1.5 mol% PEG:2000-DPPE	64.7 ± 0.1	865 ± 5
+2 mol% PEG:2000-DPPE	64.8 ± 0.1	870 ± 6
HSA	63.3 ± 0.1	820 ± 5
+0.05 mM free PEG:2000	63.4 ± 0.1	845 ± 4
+0.1 mM free PEG:2000	63.6 ± 0.1	860 ± 4
+0.15 mM free PEG:2000	63.6 ± 0.1	925 ± 3
+0.2 mM free PEG:2000	63.7 ± 0.1	960 ± 4
+0.25 mM free PEG:2000	63.8 ± 0.1	975 ± 5
+0.3 mM free PEG:2000	63.8 ± 0.1	975 ± 5

keeping with our spin-label ESR and fluorescent data (see Figs. 4a, 7b, 8). However, no distinct peaks attributable to the unfolding of specific protein regions are evident in the large DSC thermogram likely because the unfolding temperatures of the HSA domains found by ESR and Trp fluorescence do not differ appreciably.

The presence of DPPC multilayers broadens the transition, decreases ΔH to 690 kJ/mol and increases T_t by about 1°C (bottom dashed line in Fig. 9 and Table 1). The DSC results are consistent with those of ESR and fluorescence in that T_t increases. Moreover, they indicate that the protein assumes a more loosened conformation by the interaction with DPPC bilayers.

Interesting features can be observed from the DSC thermograms of HSA when PEG:2000-DPPE polymer-lipids are mixed with DPPC. In the mushroom regime at 0.5 mol%, the presence of the polymer chains at the lipid/protein interface brings ΔH back to the reference value recorded in the presence of HSA alone and increases T_t by about 1°C (see Table 1). A further addition of polymer-lipids increases both ΔH and T_t. These results clearly indicate an influence of the grafted PEG:2000 chains on the protein. This is further confirmed by DSC results reported in Table 1. In fact, dispersing HSA in a buffered solution containing free PEG:2000 results in a moderate progressive increase in T_t and even more in ΔH with increasing concentration of the free polymer.

Discussion

The interaction of albumins from different species with a variety of conventional, ungrafted phospholipid membranes has been addressed in several studies. They have mainly regarded either the effects of the proteins on the structural organization and on the molecular properties of phopholipid bilayers (Bartucci et al. 2002; Dimitrova et al. 2000; Galantai and Bardos-Nagy 2000; Wang et al. 2002, 2004) or how phospholipid model membranes influence the binding and transport properties of albumins (Pantusa et al. 2005; Galantai et al. 2000; Abreu et al. 2003). The results of the present study are concerned with the effects on HSA consequent to its interaction with mixed membranes of DPPC/PEG:2000-DPPE.

Spin-label ESR and fluorescence data indicate that the interaction of HSA with zwitterionic DPPC bilayers is weak, non-specific and does not involve tight binding. HSA adsorbs on the DPPC surface likely with the Cys-34 side. Indeed, the presence of DPPC liposomes alters the conformation of the protein region around Cys-34, favouring both a more loosened conformation of domain I and the partitioning of the *W* component between the aqueous phase and the interfacial region of lipid membranes. The partitioning is negligible at low temperature in the gel state bilayers and becomes more evident on increasing the temperature, when the lipid bilayers are in the fluid phase, where the area per polarhead is higher, and when the protein unfolds. Domains II and III are also influenced by HSA/DPPC interaction. From energy transfer evaluation of our Trp-214 data in the presence of NPA–Tyr-411 complex, it comes out that the distance between the two amino acid residues is 24 ± 1 Å in HSA (Hagag et al. 1983) and it reduces to 21 ± 1 Å in the presence of DPPC bilayers. Likely, on adsorbing on DPPC bilayer surfaces, the protein undergoes a local structural alteration so that the domain II and III come closer to each other. The attenuation of the Trp and NPA fluorescence could, therefore, be due to an intrinsic quenching by the neighbour residues in the polypeptide chain (e.g.,

residues forming S–S bridges). Globally, as evidenced by DSC results, the protein assumes a more loosened conformation on interacting with DPPC bilayers.

HSA monomer is an approximately heart-shaped molecule with overall dimensions $8 \times 8 \times 3$ nm^3 (Sugio et al. 1999) negatively charged (pI = 4.7) at pH 7.2. In the presence of terminally grafted PEG:2000 chains and gel phase DPPC bilayers, two types of protein adsorption at the liposome surfaces are predicted: primary adsorption directly at the liposome surface at low grafting density in the mushroom regime, and secondary adsorption at the periphery of the polymer-brush (Halperin 1999). The most likely explanation of the spin-label ESR and fluorescence results (see Figs. 5, 6) is that on increasing the amount of PEG-lipids mixed with DPPC through the mushroom regime, the steric lateral repulsion among the polymer chains excludes progressively the protein from the DPPC surfaces and the lipid/protein interaction reduces. Note that HSA adsorption on DPPC/PEG:2000-DPPE vesicles is also disfavoured by the electrostatic repulsion between the acidic protein and the negative charge of the liposomes conferred by the PEG:2000-DPPE polymer-lipids. The primary adsorption is completely suppressed on entering the brush regime at 1 mol% PEG:2000-DPPE as can be argued by spin-label ESR results of 5-MSL/HSA and DPPC/PEG:2000-DPPE samples. Moreover, when the content of PEG:2000-DPPE mixed with DPPC is in the brush regime, only a further reduction of the lipid induced effects on HSA are observed with ESR and fluorescence (see Figs. 5, 6) whereas DSC data indicate an influence of the polymer chains on the protein (see Fig. 9). These are clear experimental evidence of secondary HSA adsorption at the polymer brush. The influence of the polymer chains on the protein is also confirmed by DSC experiments on the protein dispersed in aqueous solution containing free PEG of the same molecular mass and at the same concentration of the grafted PEG. Both the free and grafted polymer have the same effects on the thermodynamic parameters of HSA (see Table 1). Spectroscopic studies on HSA/PEG:3500 aqueous dispersions showed that free PEG:3500 is located along the polypeptide chain of HSA through H-bonding interactions and at low concentrations (0.5 mM) stabilizes protein conformation (Ragi et al. 2005). Similarly, the residence of the protein at the periphery of the PEG:2000 brush could affect its conformation by reinforcing the intermolecular interaction, via hydrogen bonding, hydrophobic and van der Waals interactions (Rixman et al. 2003).

A progressively attenuated primary HSA adsorption on DPPC liposome surfaces has been detected by ESR using 5-PCSL, i.e., a spin-labelled lipid at the C-5 position in the sn-2 acyl chain, in sterically stabilized liposomes with PEG:2000-DPPE at mushroom content. The primary protein adsorption was completely abolished at the onset of the brush transition (Bartucci et al. 2002). The remote location of the label in the hydrocarbon region of the lipid bilayers was not suitable for detecting secondary HSA adsorption at the polymer edge. This is done here studying the effects of the polymer-lipids on the protein. Measurements of surface plasmon resonance have instead revealed that the total (both primary and secondary) HSA adsorption on distearoylphosphatidylethanolamine (DSPE) is attenuated and then almost suppressed by admixture of 1.4 and 4.7 mol% of PEG:2000-DSPE, respectively (Efremova et al. 2000).

Recent experimental studies (Price et al. 2001; Dos Santos et al. 2007) put in evidence that mechanisms other than repulsion of opsonizing proteins may be responsible for prolonged lifetime in the circulation of PEG-grafted membranes (Price et al. 2001). Indeed, it has been evidenced that as little as 0.5 mol% of PEG:2000-DSPE substantially increased plasma circulation longevity of liposomes prepared with distearoylphosphatidylcholine (DSPC) and optimal plasma circulation lifetimes is achieved with 2 mol%. At this proportion of PEG:2000-lipids the aggregation of DSPC-based liposomes was completely precluded whereas the total protein adsorption was not (Dos Santos et al. 2007).

We provided evidence that the adsorption of HSA to neutral DPPC liposome surfaces is progressively attenuated by the inclusion in the host lipid matrix of up to 2 mol% of PEG:2000-DPPE. Primary protein adsorption on zwitterionic DPPC surfaces is abolished at 1 mol% of the polymer-lipid and secondary protein adsorption to terminally grafted PEG:2000 brush persists at the highest grafting density studied.

Acknowledgments Manuela Pantusa thanks the University of Calabria for a research grant. This work was financially supported by University of Calabria.

References

Abreu MSC, Estronca LMBB, Moreno MJ, Vaz WLC (2003) Binding of a fluorescent lipid amphiphile to albumin and its transfer to lipid bilayer membranes. Biophys J 84:386–399

Bartucci R, Pantusa M, Marsh D, Sportelli L (2002) Interaction of human serum albumin with membranes containing polymer-grafted lipids: spin-label ESR studies in the mushroom and brush regimes. Biochim Biophys Acta 1564:237–242

Bosker WTE, Iakovlev PA, Norde W, Cohen Stuart MA (2005) BSA adsorption on bimodal PEO brushes. J Colloid Interface Sci 286:496–503

Carter DC, Ho JX (1994) Structure of serum albumin. Adv Protein Chem 45:152–203

Chiu GN, Bally MB, Mayer LD (2001) Selective protein interactions with phosphatidylserine containing liposomes alter the steric stabilization properties of poly(ethylene glycol). Biochim Biophys Acta 1510:56–69

De Simone F, Guzzi R, Sportelli L, Marsh D, Bartucci R (2007) Electron spin-echo studies of spin-labelled lipid membranes and free

fatty acids interacting with human serum albumin. Biochim Biophys Acta 1768:1541–1549
Dimitrova MN, Matsumura H, Dimitrova A, Neitchev VZ (2000) Interaction of albumins from different species with phospholipid liposomes. Multiple binding sites system. Int J Biol Macromol 27:187–194
Dos Santos N, Allen C, Doppen AM, Anantha M, Cox KAK, Gallagher RC, Karlsson G, Edwards K, Kenner G, Samuels L, Webb MS, Bally MB (2007) Influence of poly(ethylene glycol) grafting density and polymer length on liposomes: relating plasma circulation lifetimes to protein binding. Biochim Biophys Acta 1768:1367–1377
Du H, Chandaroy P, Hui SW (1997) Grafted poly(ethylene glycol) on lipid surfaces inhibits protein adsorption and cell adhesion. Biochim Biophys Acta 1326:236–248
Efremova NV, Bondurant B, O'Brien DF, Leckband DE (2000) Measurements of interbilayer forces and protein adsorption on uncharged lipid bilayers displaying poly(ethylene glycol) chains. Biochemistry 39:3441–3451
Fang F, Szleifer I (2006) Controlled release of proteins from polymer-modified surfaces. Proc Natl Acad Sci 103:5769–5774
Fang F, Satulovsky J, Szleifer I (2005) Kinetics of protein adsorption and desorption on surface with grafted polymers. Biophys J 89:1516–1533
Faruggia B, Picò GA (1999) Thermodynamic features of the chemical and thermal denaturations of human serum albumin. Int J Biol Macromol 26:317–323
Galantai R, Bardos-Nagy I (2000) The interaction of human serum albumin and model membranes. Int J Pharm 195:207–218
Galantai R, Bardos-Nagy I, Modos K, Kardos J, Zavodszky P, Fidy J (2000) Serum albumin-lipid membrane interaction influencing the uptake of porphyrins. Arch Biochem Biophys 373:261–270
Graceffa P, Lehrer SS (1984) Dynamic equilibrium between the two conformational states of spin-label tropomyosin. Biochemistry 23:2606–2612
Griffith OH, Jost PC (1976) Lipid spin labels in biological membranes. In: Berliner LJ (ed) Spin labeling. theory and applications. Academic Press, New York, pp 453–523
Hagag N, Birnbaum ER, Darnall DW (1983) Resonance energy transfer between cysteine-34, tryptophan-214 and tyrosine-411 of human serum albumin. Biochemistry 22:2420–2427
Halperin A (1999) Polymer brushes that resist adsorption of model proteins: design parameters. Langmuir 15:2525–2533
Hashizaki K, Taguchi H, Sakai H, Abe M, Saito Y, Ogawa N (2006) Carboxyfluorescein leakage from poly(ethylene glycol)-grafted liposomes induced by the interaction with serum. Chem Farm Bull 54:80–84
He XM, Carter DC (1992) Atomic structure and chemistry of human serum albumin. Nature 358:209–215
Jeon SI, Andrade JD (1991) Protein surface interactions in the presence of polyethylene oxide: 2. effect of protein size. J Colloid Interface Sci 142:159–166
Jeon SI, Lee JH, Andrade JD, De Gennes PG (1991) Protein surface interactions in the presence of polyethylene oxide: 1. simplified theory. J Colloid Interface Sci 142:149–158
Jost P, Griffith OH (1976) Instrumental aspects of spin labelling. In: Berliner LJ (ed) Spin labeling. theory and applications. Academic Press, New York, pp 251–272
Krishnakumar SS, Panda D (2002) Spatial relationship between the prodan site, Trp-124, and Cys-34 residues in human serum albumin and loss of structure through incremental unfolding. Biochemistry 41:7443–7452
Ladokhin AS, Jayasinghe S, White SH (2000) How to measure and analyze tryptophan fluorescence in membranes properly, and why bother? Anal Biochem 285:235–245
Lakowicz JR (1983) Principles of fluorescence spectroscopy. Plenum Press, New York
Lasic DD (1993) Liposomes: from physics to applications. Elsevier, Amsterdam
Lasic DD, Martin F (1995) Stealth liposomes. CRC Press, Boca Raton
Lasic DD, Needham D (1995) The "stealth" liposome: a prototypical biomaterial. Chem Rev 95:2601–2628
Liu X, Shang L, Jiang X, Dong S, Wang E (2006) Conformational changes of β-lactoglobulin induced by anionic phospholipid. Biophys Chem 121:218–223
Marsh D (1981) Electron spin resonance: spin labels. In: Grell E (ed) Membrane spectroscopy. Springer, Berlin, pp 51–115
Marsh D (1982) Electron spin resonance: spin label probes. In: Metcalfe JC, Hesketh TR (eds) Techniques in lipids and membrane biochemistry, vol B4/II. Elsevier, Amsterdam, B426/1–B426/44
Marsh D, Horvath LI (1989) Spin label studies of the structure and dynamics of lipids and proteins in membranes. In: Hoff AJ (ed) Advanced EPR applications in biology and biochemistry. Elsevier, Amsterdam, pp 707–752
Marsh D, Horvath LI (1998) Structure, dynamics and composition of the lipid–protein interface: perspectives from spin-labeling. Biochim Biophys Acta 1376:267–296
Marsh D, Bartucci R, Sportelli L (2003) Lipid membranes with grafted polymers: physicochemical aspects. Biochim Biophys Acta 1615:33–59
Michnik A, Michalik K, Drzazga Z (2005) Stability of bovine serum albumin at different pH. J Therm Anal Calorim 80:399–406
Muzammil S, Kumar Y, Tayyab S (1999) Molten globule-like state of human serum albumin at low pH. Eur J Biochem 266:26–32
Narazaki R, Maruyama T, Otagiri M (1997) Probing the cysteine 34 residue in human serum albumin using fluorescence techniques. Biochim Biophys Acta 1338:275–281
Norde W, Gage D (2004) Interaction of bovine serum albumin and human blood plasma with PEO-tethered surfaces: influence of PEO chain length, grafting density and temperature. Langmuir 20:4162–4167
Pantusa M, Sportelli L, Bartucci R (2005) Transfer of stearic acids from albumin to polymer-grafted lipid containing membranes probed by spin-label electron spin resonance. Biophys Chem 114:121–127
Peters T (1995) All about albumin: biochemistry, genetics and medical applications. Academic Press, San Diego
Pico GA (1997) Thermodynamic features of the thermal unfolding of human serum albumin. Int J Biol Macromol 20:63–73
Price ME, Cornelius RM, Brash JL (2001) Protein adsorption to polyethylene glycol modified liposomes from fibrinogen solution and from plasma. Biochim Biophys Acta 1512:191–205
Ragi C, Sedaghat-Herati MR, Ahmed Ouameur A, Tajmir-Riahi HA (2005) The effects of poly(ethylene glycol) on the solution structure of human serum albumin. Biopolymers 78:231–236
Ren J, Lew S, Wang Z, London E (1997) Transmembrane orientation of hydrophobic α-helices is regulated both by the relationship of helix length to bilayer thickness and by the cholesterol concentration. Biochemistry 36:10213–10220
Rixman MA, Dean D, Ortiz C (2003) Nanoscale intermolecular interaction between human serum albumin and low grafting density surfaces of poly(ethylene oxide). Langmuir 19:9357–9372
Santra MK, Banerjee A, Rahaman O, Panda D (2005) Unfolding pathways of human serum albumin: evidence for sequential unfolding of its three domains. Int J Biol Macromol 37:200–204
Shrake A, Frazier D, Schwarz FP (2006) Thermal stabilization of human albumin by medium- and short-chain *n*-alkyl fatty acid anions. Biopolymers 81:235–248
Sterk M, Hauser H, Marsh D, Gehring H (1994) Probing conformational states of spin-labeled aspartate aminotransterase by ESR. Eur J Biochem 219:993–1000

Sugio S, Kashima A, Mochizuki S, Noda M, Kobayashi K (1999) Cristal structure of human serum albumin at 2.5 Å resolution. Protein Eng 12:439–446

Szleifer I (1997) Protein adsorption on surface with grafted polymers: a theoretical approach. Biophys J 72:595–612

Wang X, Zhang Y, Wu J, Wang M, Cui G, Li J, Brezesinski G (2002) Dynamical and morphological studies on the adsorption and penetration of human serum albumin into phospholipid monolayers at the air/water interface. Colloids Surf B 23:339–347

Wang X, He Q, Zheng S, Brezesinski G, Mohwald H, Li (2004) J structural changes of phospholipid monolayers caused by coupling of human serum albumin: a GIXD study at the air/water interface. J Phys Chem B 108:14171–14177

Wetzel R, Becker M, Behlke J, Billwitz H, Bohm S, Ebert B, Hamann H, Krumbiegel J, Lassmann G (1980) Temperature behaviour of human serum albumin. Eur J Biochem 104:469–478